Selection driven tumor evolution involving non-cell autonomous environmental engineering leads to patterns of clonal expansion consistent with neutral evolution

Jack Edwards, Andriy Marusyk, David Basanta

Integrated Mathematical Oncology Department, H. Lee Moffitt Cancer Center & Research Institute, 12902 Magnolia Drive, SRB 4 Rm 24000H Tampa, Florida, 33612

Tumors arise and progress according to the laws of Darwinian evolution. *i.e.*, an interplay between mutational diversification and environmental selection. While the mutational component of somatic evolution is relatively well understood, the nature of the selection forces acting on populations of tumor cells, and how these forces are impacted by interactions between subclonal populations as they cooperate and compete for limited resources, remains poorly understood. As space is the key growth-limiting resource, both the ability to create this resource through engineering, achieved by degrading extracellular matrix, and the ability to utilize this resource effectively through maximizing proliferation, are likely to be under strong selection. While the ability to proliferate is a cell-intrinsic property, degradation of ECM is achieved through secretion of matrix-degrading enzymes, representing "public good", which can benefit both producers and non-producers. Assuming the well-established principle of evolutionary tradeoff, we used agent-based modeling to explore the interplay between engineering and consumption strategies in evolving populations of tumor cells, as well as the impact of this interplay on tumor heterogeneity and clonal composition in space and time. We found that that this interplay results in ecological succession, enabling generation of large, heterogenous and highly proliferative populations. Surprisingly, even though in our simulations both engineering and consumption strategies were under strong positive selection, their interplay led to sub-clonal architecture that could be interpreted as neutral evolution with sampling strategies commonly used in tumor genome analyses. Our results warrant more careful interpretation of inferences from sequencing cancer genomes and highlight the importance of consideration of ecological aspects of somatic evolution.

Introduction

Cancer is a disease that starts when a cell in our body breaks away from the rules of cooperation and homeostasis imposed by multicellularity and starts acting as an independent evolutionary entity. As a cell that has lost homeostatic constraints divides, its progeny (clone) acquires genetic and epigenetic alterations generating novel phenotypic variants (subclones). This subclonal diversification enables a selection for more fit variants, which can lead to evolution of malignancy through selection-driven expansion of subpopulations that have acquired hallmarks of cancers[1–6]. Sub-clonal diversification generates genetic and phenotypic Intratumor Heterogeneity (ITH), which correlates to poor prognosis and contributes to treatment failure[7,8]. Understanding the basic rules that govern the somatic evolution and how ITH is maintained

in the face of subclonal competition is the key to more effective tumor prevention and therapies[9,10].

Mathematical modelling has been used to understand the behavior of complex dynamic systems, which are difficult to intuit, such as changes in cell populations in space and time during emergence and progression of cancers. Once properly parameterized and experimentally validated, mathematical models could not only provide a deeper understanding of the complex processes, but also serve as predictive tools for therapy optimization. Ordinary Differential Equations (ODE), the most commonly used tools to model somatic evolution, typically assume well-mixed populations[11,12]. This assumption fails to account for space as a key growth limiting resource, which might have profound impact on evolutionary dynamics. Agent-based modeling tools which can consider cells as individual agents, rather than populations, can be used to account for space and spatial structures. The importance of space has been demonstrated by using agent-based models, showing that an increase in available space results in higher ITH and can affect evolutionary mode[13–15].

Epithelial tissues, which give rise to the majority of human cancers, are organized as layered structures, constrained by basal membranes and extracellular matrix (ECM)[16,17]. Carcinogenesis involves breaking from the growth limitations of epithelial layers and gaining access to the new space through degrading ECM[18]. From ecological perspective, accessing this new space constitutes niche engineering, thus we will refer to phenotypes of cancer cells which possess this ability as **engineers**[19]. ECM degradation is achieved through secretion of matrix-degrading enzymes, which require sufficiently high local concentration to achieve their effects. Since matrix degrading enzymes are secreted factors, they constitute public good, which can benefit not only engineers, but also non-engineer cells which can exploit the newly created space. Optimization of space exploitation can be achieved by increased consumption of this resource through increased proliferation rates; thus, we will refer to a phenotype that optimizes space consumption as **proliferating** phenotype. To understand eco-evolutionary dynamics resulting from selection for optimization of strategies to create (engineering) and consume (proliferating) spatial resource, we consider an abstract on-lattice grid, where spatial units are separated by degradable barriers ECM barriers.

Using a Cellular Automaton (CA) we examined eco-evolutionary dynamics of resulting from selection pressures to optimize engineering and proliferating dynamics within domains with different spatial organization[20,21]. We found that gaining access to new space through non-cell autonomous effects of engineers, dramatically increases ITH and leads to patterns of ecological succession. Surprisingly, we found that this selection-driven dynamic could lead to patterns of subclonal diversification that can be interpreted as evidence for neutral evolution, under sampling resolution commonly used in cancer genomics.

Methods

The model used a 2D on-lattice agent-based CA model, where each space in the grid is either unoccupied, blocked by a membrane, or is occupied by a living cell.

There are three classes of phenotypes in the model: basic, proliferative, and engineering. The basic cells are capable of proliferating while ignoring homeostatic signaling constraints, as long as space is available, but are incapable of accessing new space through degradation of matrix. The engineering cells proliferate at the same rates as basic cells but can provide access to new space by degrading grid barriers through secretion of matrix degrading enzymes. No single engineering cell can produce enough enzyme on its own to degrade the ECM; a substantial population of engineers local to the ECM must secrete enzymes at the same time to access new space. The proliferative cells can divide at higher rates than basic and engineering phenotypes, thus they are more effective at claiming available space, but they cannot gain access to new space on their own.

The model uses a Moore neighborhood in its algorithms[20]. Proliferation begins in the model by collecting and stochastically ordering a list of all cells. Then, one by one, each cell determines if it is fit enough to divide that timestep, and if the environment will allow the cell to divide that timestep. The model imposes a severe contact inhibition – if there is no space in a cell's neighborhood, even if the cell passed its fitness check, it will be unable to divide that timestep. Cells have a potential proliferation rate which defines its ability to proliferate if space is available. For instance, a cell with a potential proliferation rate of 75% has a 75% probability to divide at each time step, provided space is available in the neighborhood. Potential proliferation starts at 50% can be increased by mutations that optimize proliferative phenotype – up to 100% (dividing at each time step given space availability). At each time step, a cell has a 15% probability of dying, which leaves an empty space in the next timestep, enabling cell turnover within the tumor.

At each cell division, one of the following three types of mutations can occur. First, a proliferation-driving mutation, occurring at 0.07% probability, can increase cell proliferation with a randomly chosen increment of 0.01% between 10 and 20%. Second, engineering-driving mutation, occurring at 0.07% probability, bestows a cell with an engineering phenotype, enabling the mutated cell to produce a matrix-degrading enzyme at 50% probability per time step. Efficiency of engineering phenotypes can be further increased by additional engineering mutations, through increments between 10 and 20%. Based on the principle of evolutionary tradeoff, we consider engineer (ECM-producing) or proliferative phenotypes to be mutually exclusive[22]. Acquisition of engineering phenotype resets proliferation to the baseline rate of 50%. Cells have a memory effect of prior driver mutations, so that with the next switch from proliferative to engineering phenotype (and vice versa) cells a reset to the maximal previous probability of proliferation or enzyme production. Finally, a "passenger" mutation, occurring with 0.5% per time step probability, could be either entirely neutral, or slightly deleterious by decreasing probability of proliferation from 0 to 0.5%, with 0.01% increment.

In order to interrogate genetic ITH, we have recorded mutational history for each cell. Each "driver" mutational or any successive four passenger events were used in the analyses as a mutational branching point, marking a new sub-clone. Phenotypic strategies and mutational history were tracked for all the lineages over time. To define phenotypic ITH, we binned cells based

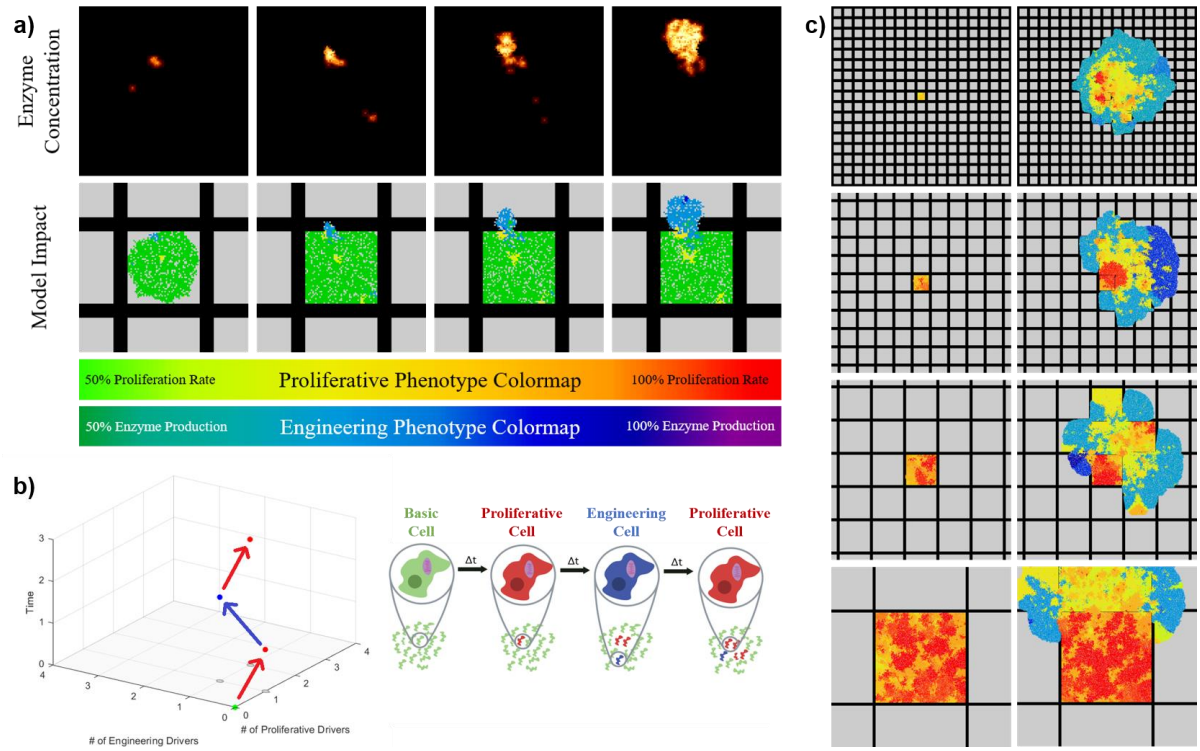

Figure 1: A collection of model rules and processes. **a)** A depiction of engineers at work in the model. For the ECM to be degraded, a sufficient concentration (~45% enzyme per lattice unit) of matrix-degrading enzyme is required near the ECM. The top images show the concentration of enzyme and the bottom images show the population of engineers producing them (with phenotypic color map below). **b)** Rules for phenotypic expression in the model. As a basic cell acquires mutations, it can only express one phenotype at a time. A sample lineage is given, where a cell's genotype is shown over time along with its expressed phenotype. **c)** Images taken from simulations of the four subdomain sizes in the model. All parameters are the same except subdomain size. The left column shows simulations where engineering failed, and the right column shows simulations where engineering succeeded.

on their proliferation and enzyme-producing phenotypes, with increments of 1%. Thus, for example, two proliferative cells representing different genetic sub-clonal branches, with proliferation probabilities of 59.1% and 59.7% would be counted as belonging to the same phenotypic subpopulation. Based on this definition of phenotypic group, there were 103 possible distinct phenotypic groups: 51 proliferative, 51 engineering, and 1 basic. Imaging in the model maps a color to a cell's phenotype and fitness as described by the aforementioned rules. The images produced by the model served as a qualitative metric for phenotypic heterogeneity within space. Muller plots, visualizing clonal dynamics, were made using EvoFreq, which is a plotting program developed by Moffitt's Integrated Mathematical Oncology department[23].

Results

We initiate simulations with 25 basic cells are seeded in the ECM surrounded sub-domain, lying in the center of the large domain, composed of the grid of sub-domains. Cell growth is constrained to the

subdomain unless ECM separating the population from the neighboring subdomain is degraded. ECM barriers can be degraded through action of engineering cells if sufficiently high concentration of ECM degrading enzymes is produced – which is a function of both numbers of engineering as well as their efficiency (**Figure 1a**). Approximately 45% enzyme per lattice unit near the ECM is the minimum concentration to degrade it. Once access to the neighboring space is achieved, the newly accessed resource can be exploited by all cell types, until all of the new space is consumed. During cell division, cells could mutationally switch their phenotype from engineering to proliferative and vice versa. Whereas these engineering and proliferative phenotypes are mutually exclusive, the mutational memory enables cells to start from the highest rates of engineering and proliferation once they switch again (**Figure 1b**). Simulations are within an 601x601 domain, separated into smaller sub-domains, ranging from 25x25 to 301x301 (shown in **Figure 1c)**, and run for 3000 timesteps, providing sufficient time for tumors where engineering was successful to completely fill the domain.

Regardless of subdomain size, we observed two scenarios defined by engineering success. In some simulations, engineering phenotype was driven to extinction, which left population confined within the sub-domains, accessed prior to extinction (failed engineering). In others, population was capable of accessing the majority or all of the sub-domains (**Figure 1c**). As a control, we examined the impact of domain size on phenotypic and clonal heterogeneity in the complete absence of engineering phenotype (**Figure S1a**). In the absence of engineering, or when engineering failed, phenotypic diversity peaked early, and

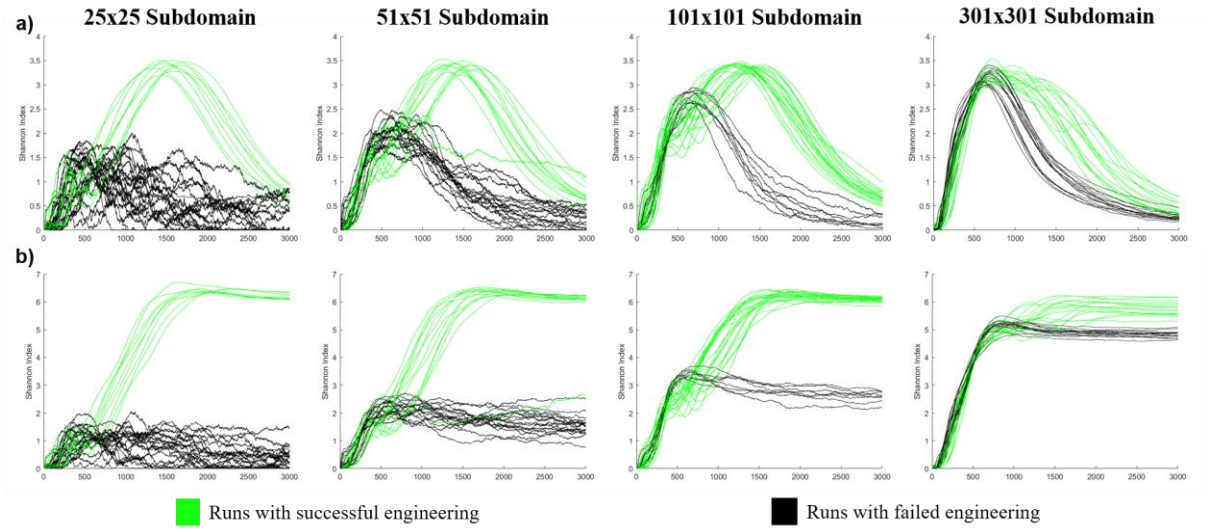

Figure 2: Heterogeneity plots from simulations in 25x25, 51x51, 101x101, and 301x301 subdomain sizes. Green lines represent simulations where engineering was a successful strategy and black lines represent runs where engineering failed. There are 30 simulations per plot, and each simulation ran for 3000 timesteps. **a)** Phenotypic heterogeneity within simulations as measured by the Shannon Index. The x-axis is time from 0 to 3000, and the y-axis is the Shannon Index from 0 to 4. **b)** Clonal heterogeneity within simulations as measured by the Shannon Index. The x-axis is time from 0 to 3000, and the y-axis is the Shannon Index from 0 to 7.

then reduced as more effective proliferators were selected. Increase in the subdomain size lead to an increase in the peak phenotypic diversity. In the presence of successful engineering, phenotypic heterogeneity peaked at later time points, but at significantly higher levels. Similar to the outcome in the absence of engineering, the phenotypic diversity decreased after reaching its peak, indicating convergent evolution towards highest proliferation rates (**Figures 2a, S1a**).

Clonal heterogeneity increased directly with subdomain size, reflecting differences in population size (**Figures 2b, S1b**). After peaking as tumor population reaches carrying capacity within spatial constrains, clonal heterogeneity remained high, with the effect more easily observed in larger subdomains. Successful engineering led to a delay in reaching maximal clonal heterogeneity but enabled populations to reach much higher levels of clonal heterogeneity. Notably, engineering limited reduction in clonal ITH, observed shortly after the peak. Therefore, environmental engineering through public goods enables tumor populations not only to gain access to space and achieve larger population size, but also increases levels of phenotypic and clonal heterogeneity.

Successful engineering was associated with noticeable patterns of phenotypic succession. After breaking the initial barrier, engineers exploited the newly accessed space, growing outwards the next barriers. As engineers continued to degrade ECM and grow outward, proliferative cells began to outcompete vestigial engineers near the core of the tumor (**Figures 3a, S2**). Once all of the ECM in the domain was removed, engineers were succeeded by proliferators, both from the expansion of pre-existing proliferative sub-clones and mutational conversion of engineers to proliferators (**Figures 3b, 3c**). Notably, this phenotypic succession was not accompanied by clonal one, as while phenotypic strategy converged toward proliferative phenotype, clonal heterogeneity

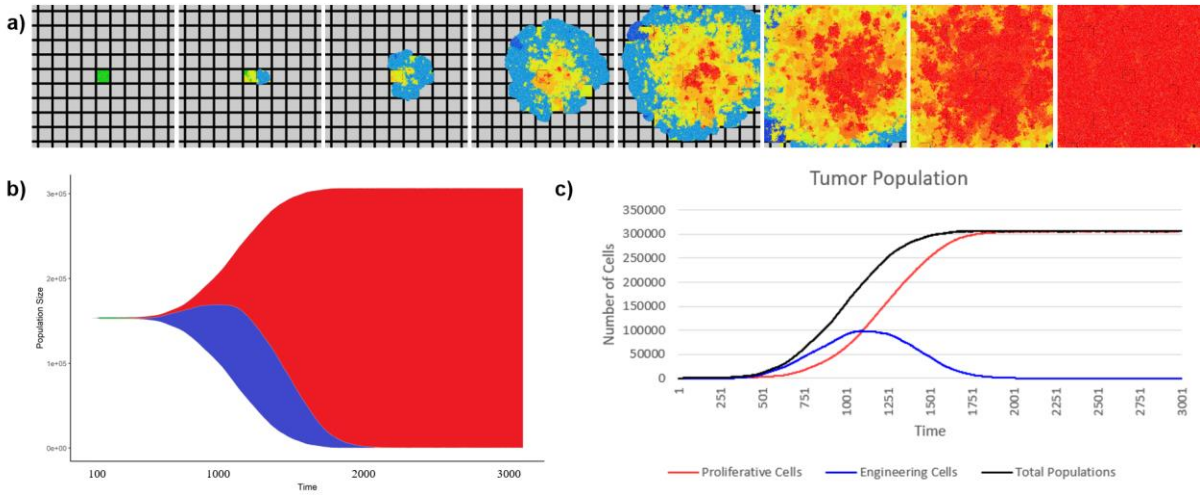

Figure 3: Patterns of ecological succession in the model. **a)** Images from the model showing engineers gaining access to new space and being succeeded by proliferative cells over time. **b)** Frequencies of basic, proliferative, and engineering cells over time. **c)** Populations of proliferative cells, engineering cells, and total tumor over time. Engineers flourish when they break out initially, and over time, proliferative cells can grow into the space created by engineers.

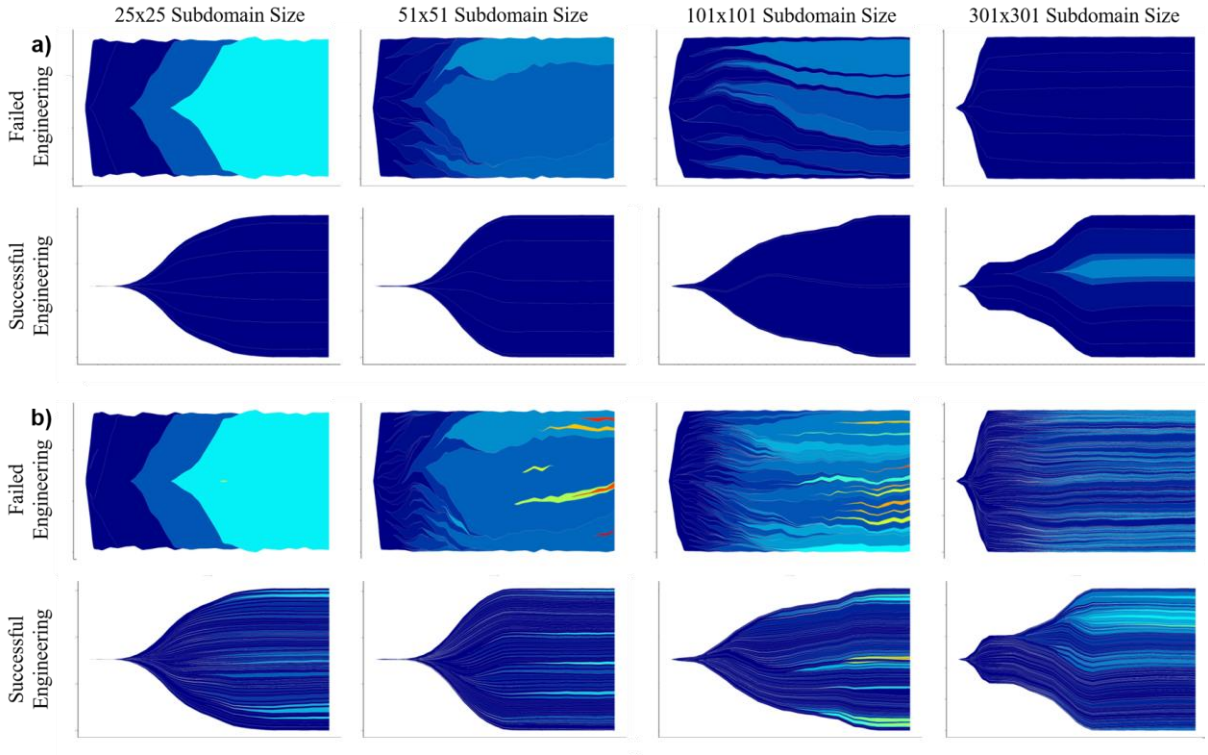

Figure 4: Muller plots created with EvoFreq. The x-axis on each plot is time, and the y-axis is population size, so the shape of the plot indicates tumor growth rate. Two simulations from each subdomain size are shown, one where engineering failed, and one where engineering succeeded. **a)** Muller plots visualized with a frequency threshold of 10%. **b)** Muller plots visualized with a frequency threshold of 1%. The color of a clonal population represents how early the clone emerged, with dark blues being the earliest and successively warmer colors indicate later clones. Clones that never had a frequency in the population greater than the threshold value are not plotted, resulting in many infrequent later clones that cause phenotypic change throughout the tumor to be invisible to visualizing.

was maintained at near peak levels. This result implies high levels of convergent evolution, when identical phenotypic solutions are reached by different subclonal lineages.

Since we recorded mutational history for each of the cell within simulation, this data enabled reconstruction of "true" (within simulations) clonal architecture, as opposed to inferences of clonal architecture, achieved through analyses of tumor genomes at a single time point. Clonal architecture was visualized using a commonly used Muller plots[23]. As large proportion of clones have low frequencies (<0.01%), they are not amenable for visualization and instead grouped with the parental clone. We chose to visualize changes in clonal architecture using 10% clonal resolution threshold (**Figure 4a**), corresponding to ~ 20x genome sequencing depth of bulk sequencing (assuming near diploid genome), and 1% clonal resolution threshold, reflecting higher resolution analyses (**Figure 4b**). In the absence of successful engineering, in small domain size we observed clear clonal succession, reflective of reconstruction of clonal evolution by cancer geneticists before availability of higher resolution tools[24]. Increase in the domain size resulted in tumors

with more complex clonal architecture, but still clear evidence of clonal expansion. Successful engineering dramatically increased clonal heterogeneity, leading to lower rates of expansion of individual sub-clones, indicative of increased clonal interference. Noticeably, increase of analysis resolution from 10% to 1% revealed more complex clonal patterns, including larger numbers of individual sub-clones as well as visual evidence of subclonal expansions (Particularly the differences in 101x101 subdomain size between **Figure 4a** and **Figure 4b**). Still, even at higher levels of resolution (**Figure S3**), in the presence of successful engineering, observed patterns of clonal expansions were largely consistent with neutral evolution despite the fact that evolutionary dynamics in our simulations was driven by explicit action of selection forces.

Discussions and Conclusions

Our study examined dynamic behavior of tumor cell populations with hypothesis-driven agent-based CA simulations, enabling explicit, unambiguous specification of rules, which shape phenotypic and clonal evolution. We found that inclusion of non-cell autonomous action of producers of "public goods" in form of environmental engineering had a profound impact on the observed dynamics, driving tumor growth, phenotypic and clonal heterogeneity. Moreover, selection-driven dynamics, involving public goods led to patterns of clonal architecture which could be interpreted as evidence of neutral evolution, based on commonly used analysis and inference tools.

Consistent with published reports of convergent evolution in cancers, where mutations with similar functional consequences are observed in distinct subclonal sub-populations[25], we observed phenotypic convergence in our simulations, as different lineages within in silico tumor were capable of finding optimal phenotypic solutions[7]. Whereas consideration of non-cell autonomous environmental engineering increased phenotypic diversity, it did not qualitatively impacted convergence.

Action of public good enabled populations of tumor cells to achieve higher levels of clonal heterogeneity. To a large extent, this effect likely reflected the ability of tumors to reach higher population size, as it was most pronounced within smaller subdomain size. However, it also enabled more effective maintenance of clonal ITH (notice lack of dip after reaching peak in green versus black lines in **Figure 2a**) – consistent with the report of maintenance of clonal heterogeneity in a mouse model of non-cell autonomous driver of tumor growth[26].

Inclusion of public good producers lead to a more complex ecological dynamics, involving local and global phenotypic successions. Ability to degrade ECM barriers led to strong selection of engineering phenotypes, as they were capable of getting priority access to the space – making engineering strategy effective at the age of tumors. However, as proliferative phenotypes were more successful in utilizing space, they eventually outcompeted engineers, leading to robustly reproducible patterns of phenotypic succession, which parallels ecological succession.

Strikingly, even though the dynamic behavior in our simulations was governed by strong selection for competing phenotypic

strategies (proliferation and engineering), inclusion of engineering resulted in subclonal architecture that could be interpreted as neutral evolution (**Figure 4a**). Analysis of genomic sequencing of tumor genomes is the major approach to reconstruct clonal evolution. Typically, these analyses are limited to a single time point (surgery), and rely on sequencing inferences, which could detect allelic frequencies present in >5% of tumor cells. Whereas regional sampling and higher sequencing depth can increase the ability to detect rare subpopulations, our results suggest that these studies might still lead to erroneous inferences of lack of selection.

It should be noted that use of hypothesis driven in silico simulations has inherent limitations. Dynamic behavior of tumor population in silico is driven by rules that are much simpler than influences experienced by tumor cells in real tumors; spatial structure used in our simulations does not faithfully recapitulate spatial architectures of normal tissues and tumors; our assumptions of mutation rates and phenotypic switching are likely to be inaccurately. On the other hand, in silico modeling enables examination of outcomes when "ground truth" of factors which govern the dynamics is known a priory – something which is not accessible not only to inferences from analyses of clinical samples, but also to experimental studies. Non-cell autonomous actions, involving public good appear to be common in tumor ecosystems, including access to vasculature nutrients, immune invasion etc[27]. Whereas out simulations only considered non-cell autonomous action in terms of accessing spatial resource, results of our simulations are likely to be generalizable to other scenarios involving public goods. We posit that consideration of ecological aspects of cancer evolution, as well as integration of mathematical modeling with experimental studies and analyses of clinical samples are essential to properly understand clonal evolution – which is a prerequisite to the development of successful strategies to prevent and eradicate cancers.

Acknowledgements

We would like to thank the Summer Program for the Advancement of Research Knowledge (SPARK) at Moffitt Cancer Center for sponsoring JE and the Integrated Mathematical Oncology Department at Moffitt for hosting this research project. We would also like to thank Dr. Joel Brown for discussions and ideas.

References

(1) Nowell, P. The Clonal Evolution of Tumor Cell Populations. *Science* **1976**, *194* (4260), 23–28. https://doi.org/10.1126/science.959840.

(2) Greaves, M.; Maley, C. C. Clonal Evolution in Cancer. *Nature* **2012**, *481* (7381), 306–313. https://doi.org/10.1038/nature10762.

(3) Axelrod, R.; Axelrod, D. E.; Pienta, K. J. Evolution of Cooperation among Tumor Cells. *Proc. Natl. Acad. Sci.* **2006**, *103* (36), 13474–13479. https://doi.org/10.1073/pnas.0606053103.

(4) Korolev, K. S.; Xavier, J. B.; Gore, J. Turning Ecology and Evolution against Cancer. *Nat. Rev. Cancer* **2014**, *14* (5), 371–380. https://doi.org/10.1038/nrc3712.

(5) Hanahan, D.; Weinberg, R. A. The Hallmarks of Cancer. *Cell* **2000**, *100* (1), 57–70. https://doi.org/10.1016/S0092-8674(00)81683-9.

(6) Hanahan, D.; Weinberg, R. A. Hallmarks of Cancer: The Next Generation. *Cell* **2011**, *144* (5), 646–674. https://doi.org/10.1016/j.cell.2011.02.013.

(7) Gerlinger, M.; Rowan, A. J.; Horswell, S.; Larkin, J.; Endesfelder, D.; Gronroos, E.; Martinez, P.; Matthews, N.; Stewart, A.; Tarpey, P.; et al. Intratumor Heterogeneity and Branched Evolution Revealed by Multiregion Sequencing. *N. Engl. J. Med.* **2012**, *366* (10), 883–892. https://doi.org/10.1056/NEJMoa1113205.

(8) Swanton, C. Intratumor Heterogeneity: Evolution through Space and Time. *Cancer Res.* **2012**, *72* (19), 4875–4882. https://doi.org/10.1158/0008-5472.CAN-12-2217.

(9) Basanta, D.; Anderson, A. R. A. Exploiting Ecological Principles to Better Understand Cancer

Progression and Treatment. *Interface Focus* **2013**, *3* (4), 20130020. https://doi.org/10.1098/rsfs.2013.0020.

(10) Sottoriva, A.; Kang, H.; Ma, Z.; Graham, T. A.; Salomon, M. P.; Zhao, J.; Marjoram, P.; Siegmund, K.; Press, M. F.; Shibata, D.; et al. A Big Bang Model of Human Colorectal Tumor Growth. *Nat. Genet.* **2015**, *47* (3), 209–216. https://doi.org/10.1038/ng.3214.

(11) Altrock, P. M.; Liu, L. L.; Michor, F. The Mathematics of Cancer: Integrating Quantitative Models. *Nat. Rev. Cancer* **2015**, *15* (12), 730–745. https://doi.org/10.1038/nrc4029.

(12) Gatenby, R. A.; Gillies, R. J. A Microenvironmental Model of Carcinogenesis. *Nat. Rev. Cancer* **2008**, *8* (1), 56–61. https://doi.org/10.1038/nrc2255.

(13) Noble, R.; Burri, D.; Kather, J. N.; Beerenwinkel, N. *Spatial Structure Governs the Mode of Tumour Evolution*; preprint; Cancer Biology, 2019. https://doi.org/10.1101/586735.

(14) West, J.; Schenck, R. O.; Gatenbee, C.; Robertson-Tessi, M.; Anderson, A. R. A. *Tissue Structure Accelerates Evolution: Premalignant Sweeps Precede Neutral Expansion*; preprint; Cancer Biology, 2019. https://doi.org/10.1101/542019.

(15) Chkhaidze, K.; Heide, T.; Werner, B.; Williams, M. J.; Huang, W.; Caravagna, G.; Graham, T. A.; Sottoriva, A. *Spatially Constrained Tumour Growth Affects the Patterns of Clonal Selection and Neutral Drift in Cancer Genomic Data*; preprint; Bioinformatics, 2019. https://doi.org/10.1101/544536.

(16) Bissell, M. J.; Radisky, D. Putting Tumours in Context. *Nat. Rev. Cancer* **2001**, *1* (1), 46–54. https://doi.org/10.1038/35094059.

(17) Bissell, M. J.; Radisky, D. C.; Rizki, A.; Weaver, V. M.; Petersen, O. W. The Organizing Principle: Microenvironmental Influences in the Normal and Malignant Breast. *Differentiation* **2002**, *70* (9–10), 537–546. https://doi.org/10.1046/j.1432-0436.2002.700907.x.

(18) Cawston, T. E.; Wilson, A. J. Understanding the Role of Tissue Degrading Enzymes and Their Inhibitors in Development and Disease. *Best Pract. Res. Clin. Rheumatol.* **2006**, *20* (5), 983–1002. https://doi.org/10.1016/j.berh.2006.06.007.

(19) Lloyd, M. C.; Cunningham, J. J.; Bui, M. M.; Gillies, R. J.; Brown, J. S.; Gatenby, R. A. Darwinian Dynamics of Intratumoral Heterogeneity: Not Solely Random Mutations but Also Variable Environmental Selection Forces. *Cancer Res.* **2016**, *76* (11), 3136–3144. https://doi.org/10.1158/0008-5472.CAN-15-2962.

(20) Margolus, N. Cellular Automata Machines. 27.

(21) Poleszczuk, J.; Enderling, H. A High-Performance Cellular Automaton Model of Tumor Growth with Dynamically Growing Domains. *Appl. Math.* **2014**, *05* (01), 144–152. https://doi.org/10.4236/am.2014.51017.

(22) Townsend, C. R.; Begon, M.; Harper, J. L. *Essentials of Ecology. [Electronic Resource]*., 3rd ed.; John Wiley & Sons, Ltd., 2009.

(23) Gatenbee, C. D.; Schenck, R. O.; Bravo, R. R.; Anderson, A. R. A. EvoFreq: Visualization of the Evolutionary Frequencies of Sequence and Model Data. *BMC Bioinformatics* **2019**, *20* (1), 710. https://doi.org/10.1186/s12859-019-3173-y.

(24) Weinberg, R. A. *The Biology of Cancer*; Garland Science, 2007.

(25) Ardaševa, A.; Gatenby, R. A.; Anderson, A. R. A.; Byrne, H. M.; Maini, P. K.; Lorenzi, T. *A Mathematical Dissection of the Adaptation of Cell Populations to Fluctuating Oxygen Levels*; preprint; Cancer Biology, 2019. https://doi.org/10.1101/827980.

(26) Marusyk, A.; Tabassum, D. P.; Altrock, P. M.; Almendro, V.; Michor, F.; Polyak, K. Non-Cell-Autonomous Driving of Tumour Growth Supports Sub-Clonal Heterogeneity. *Nature* **2014**, *514* (7520), 54–58. https://doi.org/10.1038/nature13556.

(27) Tabassum, D. P.; Polyak, K. Tumorigenesis: It Takes a Village. *Nat. Rev. Cancer* **2015**, *15* (8), 473–483. https://doi.org/10.1038/nrc3971.